Monthly Notices
of the
ROYAL ASTRONOMICAL SOCIETY

Mon. Not. R. Astron. Soc. **406,** 1140–1145 (2010) doi:10.1111/j.1365-2966.2010.16741.x

Application of Double Beltrami states to solar eruptions

D. Kagan[1⋆] and S. M. Mahajan[2⋆]

[1]*Astronomy Department, University of Texas at Austin, Austin, TX 78712-0259, USA*
[2]*Institute for Fusion Studies, The University of Texas at Austin, Austin, TX 78712-0262, USA*

Accepted 2010 March 25. Received 2010 March 10; in original form 2009 August 13

ABSTRACT

We show that the general class of Double Beltrami (DB) states, which are the lowest energy equilibria of Hall magnetohydrodynamics, can have characteristics similar to those of active regions in the solar corona and is capable of undergoing a catastrophe that can cause a solar eruption, such as a flare or coronal mass ejection (CME). We then show that the qualitative evolution of the DB state is consistent with that of a solar eruption. Finally, we make two quantitative comparisons of DB states to CMEs, which are the simplest result of the catastrophe. First, we show that the DB expansion by a factor of 1–2 before the catastrophe is consistent with the increase in the height of the leading edges of Large-Angle Spectrometric Coronagraph (LASCO C1) CMEs in the quasi-equilibrium stage. Secondly, we use the assumption that DB states are randomly chosen from the allowed phase space of coronal structures to predict that the probability of a coronal structure erupting is 0.046. Identifying active regions with DB states and using observational constraints to estimate that the state is replaced every 60 min by emerging loops results in a CME rate of 11 d^{-1}, which is in reasonable agreement with the actual rate of about 6 d^{-1} at solar maximum.

Key words: Sun: corona – Sun: coronal mass ejections (CMEs) – Sun: flares – Sun: surface magnetism.

1 INTRODUCTION

Sudden and catastrophic events such as solar flares, coronal mass ejections (CMEs) and erupting prominences are common in the solar corona. These events probably occur too rapidly for energy injection from the photosphere to drive them directly (Krall, Chen & Santoro 2000); they may instead occur when energy, stored over time in the coronal magnetic field, is rapidly released. Despite years of study, there is still no consensus as to what mechanism is behind these eruptive events.

One method for modelling solar eruptions is to assume an initial ideal magnetohydrodynamic (MHD) equilibrium and examine if a breakdown of the equilibrium can harness enough energy to produce an eruptive event. Many such equilibria are not energetically favourable; small perturbations, then, can drive the system to a new relaxed, lower energy equilibrium. The only equilibrium that is truly stable is the most likely equilibrium, found by minimization of the energy subject to topological constraints.

In MHD, the simplest fluid model for plasma physics, it can be shown that the minimum energy static ($V = 0$) equilibrium is the force-free magnetic field (Woltjer 1958):

$$\nabla \times \boldsymbol{B} = \lambda \boldsymbol{B} \tag{1}$$

where λ is a constant determined by the ratio of energy to the magnetic helicity, the latter being the topological invariant of ideal MHD. Fitting a force-free field to magnetic field measurements is a commonly used practice in modelling coronal structures.

While the force-free model of MHD is excellent at modelling equilibrium structures, it cannot account for the breakdown of these equilibria associated with changes (via reconnection, for instance) in the field topology. Such a change must occur, because an open (potential) magnetic field that results from a reconnection event has a higher magnetic energy than any corresponding initial closed field (Aly 1991; Sturrock 1991); no ideal MHD process can drive such an eruption.

Most models assume that eruptive events are driven by the reconnection of magnetic fields due to non-ideal effects like resistivity; an appropriate field geometry that can produce a reconnection event is assumed. In two standard models, initial equilibrium is assumed to be consisting, respectively, of flux ropes and multipolar magnetic fields; the latter situation defines the so-called breakout model (Forbes et al. 2006); the pre-eruption coronal structures, however, may have neither of these configurations. In addition, collisional resistivity is not large enough in the corona to produce fast reconnection. Therefore, MHD models of solar eruptions require the presence of 'anomalous' resistivity and special assumptions about the magnetic field topology in the corona.

Because of high conductivity, the Hall effect is more important than resistivity in the solar corona. It can lead to fast reconnection by providing small-scale fields that dissipate more quickly

⋆E-mail: kagan@astro.as.utexas.edu (DK); mahajan@mail.utexas.edu (SMM)

(Bhattacharjee 2004); it can also lead to the formation of fast flows from turbulent magnetic fields using the reverse dynamo mechanism (Mahajan et al. 2005), and the formation of coronal structures from an initial upflow into the corona, including the relatively fast flows observed in coronal loops (Mahajan et al. 2001). These successes indicate that Hall MHD may allow the construction of a successful 'loss of equilibrium' model for catastrophic events without making the special assumptions about topology as the flux rope and breakout models do.

This paper, investigating the possible role of Hall effect in solar eruptions, is organized as follows. In Section 2, we first describe the most likely equilibrium accessible to Hall MHD, the Double Beltrami (DB) State, and then show that DB states can suffer catastrophic loss of equilibrium under solar coronal conditions. In Section 3, we compare the characteristics of the DB catastrophe with those of solar eruptions and compare the predicted expansion during the catastrophe with observed CME kinematics. In Section 4, we calculate the rate of CMEs resulting from the DB model using a phase-space argument and compare it with the observed rate. Finally, in Section 5, we summarize our conclusions and discuss possible future work.

2 DOUBLE BELTRAMI STATES

The most likely equilibrium in Hall MHD results from the minimization of energy E while the magnetic helicity (electron helicity) h_e and the generalized helicity (ion helicity) h_i are held constant. The resulting equilibrium DB state has magnetic field $\boldsymbol{B}$ and velocity field $\boldsymbol{V}$ that consist of a sum of two simple Beltrami fields on two different scales (Mahajan & Yoshida 1998):

$$\boldsymbol{B} = C_L \boldsymbol{G}_L + C_S \boldsymbol{G}_S \tag{2}$$

$$\boldsymbol{V} = (\lambda + \widetilde{a}) C_L \boldsymbol{G}_L + (\mu + \widetilde{a}) C_S \boldsymbol{G}_S, \tag{3}$$

where the G fields satisfy the Beltrami equation (1). Note that $\boldsymbol{B}$ and $\boldsymbol{V}$ are dimensionless, as they have been normalized to some magnetic field B_0 and the corresponding Alfvén velocity. The constants $C_{L,S}$ are the amplitudes of the large and small-scale fields that have characteristic inverse scalelengths λ and μ ($\widetilde{a}$ is a parameter that may be calculated from these scalelengths).

2.1 Breakdown of Double Beltrami equilibria

The DB equilibrium has more energy available to drive an eruptive event than the linear force-free state. It can undergo a catastrophe converting magnetic energy into kinetic energy, thus, simulating one of the defining features of an eruptive event. Ohsaki et al. (2002, henceforth OSYM) found that a sequence of slowly varying DB equilibria constrained by the invariants can, indeed, terminate in a catastrophe; at the catastrophe boundary, the amplitude of the small scale vanishes tending to (formally) becoming imaginary. OSYM found that the removal of the small scale can occur if the system energy exceeds a critical energy determined by the two helicities:

$$E > E_c \equiv 2(\sqrt{h_e h_i} - h_e) \tag{4}$$

The result that the DB state can undergo a catastrophe makes it suitable as a possible state from which a solar eruption could occur. However, in order to construct a model of solar eruptive events, we must identify an evolutionary path for the four parameters that define a DB state in which the initial state has properties that correspond to those of coronal structures and the final state has the defining properties of an eruptive event.

2.2 Observational constraints on the initial state

To set up the machinery for a DB model to simulate observations, we normalize the DB states as follows. We normalize the magnetic field $\boldsymbol{B}$ to the macroscopic field of an observed coronal structure (this sets $C_L = 1$) and the velocity $\boldsymbol{V}$ to the corresponding Alfvén speed. The normalizing speed is chosen to be the Alfvén speed based on the large-scale field alone; this is very close to the true Alfvén speed in our parameter region of interest.

Observations of the solar corona constrain the energy E, large-scale wavenumber λ and large-scale normalized velocity $v \equiv V_L/v_A$ of the initial state. The maximum flow velocities commonly seen in loops are generally about $100\,\mathrm{km\,s^{-1}}$ (Kjeldseth-Moe & Brekke 1998; Fredvik et al. 2002), while the Alfvén speed for flux ropes in the solar corona (which have $B \approx 10\,\mathrm{g}$, $n \approx 10^8\,\mathrm{cm^{-3}}$) is approximately $2000\,\mathrm{km\,s^{-1}}$. This requires that $v \approx .01 \ll 1$. Now we look at the energetics of a typical eruptive event. A catastrophe can only occur with $v \ll 1$, if $E - 1 \gg 1$ or $E - 1 \ll 1$; i.e., if almost all of the energy is in the macroscopic magnetic field or almost all is outside it. The energy of solar flares is consistent with a pre-catastrophe situation in which the loop energy lies primarily in the macroscopic magnetic field. This restricts the realistic region for the initial state to $E - 1 \ll 1$, $v \ll 1$, where $\lambda \ll 1$, $\mu \gg 1$ and $C_S \ll 1$.

We now calculate the fields and invariants for the region of interest; the expressions are simplified greatly by assuming $\lambda \ll \mu^{-1}$; this implies that $\widetilde{a} \approx 1/\mu \approx v$ for typical coronal structures (OSYM). The size of typical structures in the corona is approximately 1 Mm (i.e., about one solar radius), while the Hall scale is typically about 1 m in the corona. This allows us to estimate $\lambda \approx 10^{-6}$ for these structures. Flows in the corona have typical velocities of tens of $\mathrm{km\,s^{-1}}$, while the Alfvén speed in the Corona is of order $1000\,\mathrm{km\,s^{-1}}$; this sets $v \approx \mu^{-1} \approx 0.01$. So our assumption that $\lambda \ll \mu^{-1}$ is justified for typical coronal structures.

The invariants and fields are

$$E \approx 1, \tag{5}$$

$$h_e \approx 1/\lambda, \tag{6}$$

$$h_i - h_e \approx C_S^2 \mu^3, \tag{7}$$

$$\boldsymbol{B} \approx \boldsymbol{G}_L, \tag{8}$$

$$\boldsymbol{V} \approx \mu^{-1} \boldsymbol{G}_L + \mu C_S \boldsymbol{G}_S. \tag{9}$$

The magnetic field is mostly large scale and close to being force-free. The velocity field is small in magnitude but exists on both large and small scales, and is consistent with the presence of observed slow flows on large-scales as well as small-scale turbulence.

Because $h_i - h_e \ll h_i$, the critical energy may be approximated as

$$E_c = 2(h_e - \sqrt{h_e h_i}) \approx h_i - h_e \approx C_S^2 \mu^3. \tag{10}$$

A catastrophe can occur if $C_S^2 \mu^3 < 1$.

2.3 Energy produced by the catastrophe

As the system approaches the catastrophe while conserving the invariants, the macroscopic magnetic field and velocity change, as do the amplitudes C_L and C_S and the inverse scalelengths λ and μ. At the catastrophe, $C_S = 0$, and the field is entirely macroscopic. We now test whether the catastrophe produces enough energy to

drive an eruptive event. We will use uppercase Greek letters for parameters at the catastrophe. At the critical point, the large-scale Λ is given by (OYSM)

$$\Lambda = \frac{E + \sqrt{E^2 - E_c^2}}{2h_e}. \tag{11}$$

Using this equation, it is then straightforward to calculate the macroscopic velocity at the catastrophe (in Alfvén units):

$$U^2 = \frac{E - \sqrt{E^2 - E_c^2}}{2}. \tag{12}$$

The maximum velocity producible by the DB model occurs at $E_c = 1$, and with $E \approx 1$, it is $U = 1/\sqrt{2}$. At this velocity, half of the magnetic energy has transformed into kinetic energy.

3 COMPARISON WITH OBSERVATIONS

In this section, we attempt to justify the model by comparing the properties of the initial and final DB states, respectively, with the initial conditions in the corona and final conditions observed in a solar eruptive event.

3.1 Eruptive velocities

First, we must make a comparison of the observed velocities of eruptive events with those predicted at the catastrophe. Flux ropes in active regions in the solar corona have Alfvén speeds of approximately 2000 km s^{-1} (Chen 2001); the DB catastrophe can produce a final velocity of $v_A/\sqrt{2} \approx 1400\,\mathrm{km\,s^{-1}}$. The vast majority of CMEs have peak velocities less than 1500 km s^{-1} (Schwenn et al. 2006). Therefore, the most energetic DB catastrophes should be able to produce enough energy to create CMEs; less energetic DB catastrophes can produce smaller flares or prominence eruptions.

3.2 Changes in the DB parameters

Near the catastrophe, $h_e \approx 1/\lambda$ and $E \approx 1$, and λ behaves as

$$\frac{\Lambda}{\lambda} \approx \frac{1 + \sqrt{1 - E_c^2/E^2}}{2}. \tag{13}$$

The minimum ratio between the final and initial large-scale size is 1/2, at $E = E_c$; for $E > E_c$, the ratio will be closer to 1. So λ decreases slightly as the system moves towards the critical point; therefore the large scale increases in size by a small amount. The change from the initial to the final lengthscales corresponds well with known properties of coronal loops (initial), in which the sides tend to repel due to the Shaforonov hoop stress, and the properties of CMEs and prominences (final) that expand and move upward as they approach the moment of eruption.

Next, we consider the value of C_L (which is also the amplitude of B_L). For the region of interest, $h_e \approx C_L^2/\lambda$. Since h_e is invariant, $C_L \propto \sqrt{\lambda}$. The large scale magnetic field, thus, drops as the system approaches the catastrophe. The decrease in the magnitude of the macroscopic magnetic field fits well with what we see in eruptive events; magnetic energy is converted into kinetic energy or radiation.

Next, we consider the changes in the small-scale parameters. At the catastrophe point, the small-scale amplitude is 0, because it is there that the DB state is converted to a purely macroscopic state. The small scalelength $1/\mu$ grows to a value close to the Hall scale (from an initial size about 100 times smaller). It is possible that this small-scale size corresponds to the width of a current sheet produced in the DB catastrophe; most models of solar reconnection assume that fast reconnection is mediated by the presence of a small-scale field at approximately the Hall scale. Because neither the DB state nor the large-scale final field are exactly force-free (due to the presence of a non-zero flow velocity), the DB model can accommodate the presence of current sheets. However, it is unnecessary to invoke a current sheet to produce an eruptive event in the DB catastrophe, because it transforms magnetic energy to kinetic energy without assumed dissipation.

3.3 Result of the catastrophe

While the general features of the post-catastrophe state discussed previously can be predicted using the DB equilibrium model, detailed features of this state (the detailed field geometry, the fate of the kinetic energy) cannot. The region modelled by the DB state may erupt off the solar surface (if its velocity exceeds the solar escape speed); this may correspond to a CME. It is also possible that the energetic plasma will be confined by the local magnetic field; this is especially likely to occur if the eruptive event has low energy compared to that in the local magnetic field ($U \ll 1$). If this occurs, most of the kinetic energy is likely to be converted to heat and radiated away, resulting in a non-eruptive flare.

Because the large-scale velocity field varies within the DB region, the results of the catastrophe may vary from place to place; a CME and a flare could result from the same catastrophe. This variation may also result in the formation of small-scale structures such as current sheets. Investigation of these questions is beyond the scope of this paper. However, it is possible to make two quantitative comparisons between the DB model and CMEs; these tests will serve as indicators of the applicability of DB states to solar eruptions in general.

3.4 CME kinematics

The DB model predicts that the scale size of the state will increase by a factor of 2 or less before the catastrophe occurs; furthermore, the higher the final energy of the eruptive event, (in Alfvénic units) the greater the expansion. The kinematics of CMEs, which often display a quasi-equilibrium stage prior to eruption, provides an excellent observational test for this pre-catastrophe expansion.

Most CMEs display a three-part kinematic history (Zhang et al. 2001). The first may be thought of as a quasi-equilibrium stage during which structures rise slowly, with little change in speed. The second phase is associated with rapid acceleration; it is in this stage that the CME nearly reaches its final velocity. Finally, the CME drifts at near-constant speed, affected mostly by drag forces.

Because the first stage corresponds well with the quasi-equilibrium model, measuring the height at which acceleration begins in comparison with the height at which the leading edge of the CME is first viewed, and then finding the ratio of the heights, will be a test of the theory. We use CME events from the LASCO C1 CME data base (which can be found at http://solar.scs.gmu.edu/research/cme_c1/) to test the prediction (Fig. 1). Only CMEs with a clear quasi-equilibrium stage and a clearly visible leading edge are included in the sample.

The figure indicates that most of the CMEs meet the criterion of a two-fold or smaller expansion, and the others do not exceed the criterion by much. Even these anomalous CMEs are not necessarily in contradiction with the model, because the height of the leading edge is only one dimension of the coronal field; the others could expand less, leading to a smaller average value of λ. We do not observe the

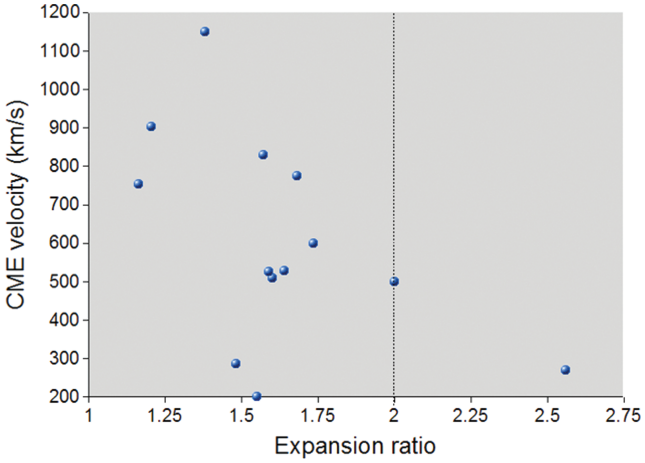

Figure 1. A comparison of the quasi-equilibrium expansion rate of CMEs to their final velocity. The CME data was taken from the LASCO C1 data base.

expected correlation (13) between the CME speed and the amount of expansion. This discrepancy may be due to the variation in the Alfvén speeds at the locations of the CMEs; the predicted relationship is between *normalized* velocity and expansion ratio. CME kinematics are therefore consistent with the model, although more observations (with approximate measures of the Alfvén speed) are needed.

4 CALCULATING THE RATE OF CMEs

If DB states that form in the solar corona are chosen randomly from possible coronal states, and eruptions are independent events, the rate at which a catastrophic eruption occurs in the solar corona R_C can be calculated from the rate R_P at which new coronal states form:

$$R_C = \frac{A_C}{A_D} R_D. \tag{14}$$

Here A_C is the phase-space area of catastrophe-prone realistic DB states and A_D is the phase-space area of all realistic DB states. Because the simplest result of a DB catastrophe is a CME, and CMEs are the most violent and visible solar eruptive events, we choose to estimate the CME rate rather than that for some other eruptive event.

4.1 The predecessor and its formation rate

To calculate the predicted rate of CMEs, it is necessary to specify a structure on the Sun that corresponds to the DB state; the CME is then hypothesized to be the result of the breakdown of equilibrium that occurs if the structure is catastrophe prone. In doing so, we assume that all catastrophe-prone states eventually undergo catastrophe, and that the formation and ejection rate of catastrophe-prone states is approximately the same.

About 85 per cent of CMEs are associated with active regions (Dasso et al. 2005) (the rest may be associated with ones that recently appeared or disappeared), and CMEs are large-scale events that cover entire active regions; therefore, it makes sense to identify DB states with active region configurations. The time-scale for large-scale changes in an active region is generally on the order of days, but it can be as short as 1 h during times of heightened activity, when flares or CMEs occur. It therefore makes sense to assume that the DB state in the active region, associated with its large-scale structure, is continually modified by emerging coronal loops; the result is that a new DB state is formed every hour in an active region, and the emergence (and removal) of flux can move the state towards or away from a CME-prone state. The small 'distance' that a catastrophe-prone state must travel in phase space to reach a loss of equilibrium means that the catastrophe is likely to occur quickly, before a new DB state replaces the old one.

We can estimate upper and lower limits on the time-scale on which the DB state is replenished. A maximum time-scale for the formation of CME precursors may be found by examining successive CMEs from the same region; the precursor formation rate for active regions must be greater than the rate at which successive CMEs can occur in the regions of greatest activity. The recurrence time for CMEs in National Oceanic and Atmospheric Administration (NOAA) active region 9236 was found to be about 4.6 h, while the smallest time difference was shorter (Gopalswamy et al. 2006). A minimum time-scale may be found by calculating the radiative cooling time for typical coronal loops; any major change cannot happen faster than the time required for a loop to destabilize, about 10 min (Kjeldseth-Moe & Brekke 1998). So a 1 h estimate for DB state emergence in an active region seems reasonable.

To allow for more accurate results with less net variability, all parameters will be calculated at solar maximum, when there are typically 10 active regions on the Sun (this was obtained from http://www.solarmonitor.org by sampling days near maximum). In addition, the sunspot number on the Sun is about 100–150 at solar maximum, which corresponds to 10 active regions if the number of solitary sunspots is low. On the whole Sun, then, the resulting rate of production of CME predecessors is 240 d^{-1}.

4.2 Phase-space areas

The projection of the phase space of DB states that is relevant to the probability of catastrophe is two-dimensional, because the probability of catastrophe and the CME velocity provided by the catastrophe depend only on E_C/E, and for the regime of interest, $E_C/E \approx C_S^2\mu^3$. Therefore, we must specify the ranges of C_S and μ that fall into A_C and A_D.

The value of C_S cannot be constrained by any known observation. In contrast, the value of the small scale $\lambda_S \approx 1/v_0$, since all predecessor velocities are very sub-Alfvénic; therefore, constraints are possible due to limitations on the initial velocity. For the initial state, the boundaries of the region are marked by just the values of μ corresponding to the maximum and minimum of v (the velocity of flows in the predecessor), and the unknown bounds of C_S. For the final state, the bounds are

$$2U_h\sqrt{1-U_h^2} > C_S^2\mu^3 > 2U_l\sqrt{1-U_l^2}, \tag{15}$$

where U_h is the maximum critical velocity that corresponds to a CME and U_l is the minimum critical velocity.

The initial state boundaries are just the boundaries in $v \approx 1/\mu$, while the ratio of $E_C/E \approx C_S^2\mu^3$ values is the same for all C_S. Therefore, a calculation of the logarithmic areas eliminates C_S and allows a prediction of the CME production rate. The resulting estimates of the phase-space areas are

$$A_C = \left(\log\frac{C_{S,h}}{C_{S,l}}\right)\left[\left(\log\left(\frac{U_h}{U_l}\right) + .5\log\left(\frac{1-U_h^2}{1-U_l^2}\right)\right]\right., \tag{16}$$

$$A_D = \left(\log\frac{C_{S,h}}{C_{S,l}}\right)\left(3\log\frac{v_h}{v_l}\right). \tag{17}$$

If the DB model is a good model for eruptive solar events, the highest velocity CME should correspond to the maximum catastrophe velocity $U_{\rm h} = 1/\sqrt{2}$. This relation simplifies the second term of A_C yielding the phase-space ratio:

$$\frac{A_C}{A_D} = \frac{\log(V_{\rm h}/V_{\rm l}) - .5\log(2 - (V_{\rm l}/V_{\rm h})^2)}{3\log(v_{\rm h}/v_{\rm l})}. \quad (18)$$

Because only velocity ratios appear in the final expression, we replaced U (velocity in Alfvén units) with $V \equiv U v_{\rm A}$ (final velocity in km s^{-1}) in all terms.

4.3 The CME energy budget

In a CME event, a large mass of plasma is lifted against gravity, is accelerated to high speed and is generally accompanied by large bursts of radiation and showers of energetic particles. In order to account for observed CMEs, a loss of equilibrium in the DB state must provide enough energy to produce all of these events, that is,

$$E_{\rm db} = E_{\rm cme} + E_r + E_p. \quad (19)$$

The energy $E_{\rm db}$ produced by this catastrophe is $0.5U^2$ in normalized units; in physical units, it is $0.5M(U v_{\rm A})^2$. The energy $E_{\rm cme}$ needed to produce the 'CME' alone equals the sum of the kinetic energy of the CME measured far from the Sun and the gravitational potential energy difference between the solar surface and infinity:

$$E_{\rm cme} = \frac{1}{2}M v_{\rm m}^2 + \frac{G{\rm M}_\odot M}{{\rm R}_\odot}. \quad (20)$$

Here $v_{\rm m}$ is the measured velocity of a CME far from the Sun. The extra-CME energy is in the form of radiation and may be estimated as $E_r \approx 0.5E_{\rm cme}$ (Emslie et al. 2005; Dennis et al. 2006). The energy carried by high-energy particles, accelerated by the CME shocks, has been estimated to be $E_p \approx 0.1E_{\rm cme}$ (Mewaldt et al. 2005). Using these estimates, the resulting equation for the catastrophe velocity V in terms of the observed CME velocity $v_{\rm m}$ comes out to be

$$V({\rm km\,s^{-1}}) = \sqrt{1.6\left[v_{\rm m}^2 + (873\,{\rm km\,s^{-1}})^2\right]}. \quad (21)$$

This equation is really a test for the validity of the DB model to simulate the CMEs; the measured velocity $v_{\rm m}$ pertaining to observed CMEs and critical V predicted for DB states must be approximately equal.

4.4 Velocity ranges for the initial and final states

The phase-space ratio can be calculated using the minimum and maximum values of the velocity of precursors and the minimum and maximum values of the peak CME velocities. As mentioned above, the maximum velocity of coronal flows in active regions is approximately 100 km s^{-1}. Determining a minimum velocity for coronal flows is difficult, because the uncertainty in Doppler measurements is generally on the order of 5 km s^{-1} for the strongest lines. We will conservatively assume that the minimum velocity of coronal flows is 5 km s^{-1}; thus the range of initial speeds is 5–100 km s^{-1}. CME velocities range about 100–1500 km s^{-1}, with a mean velocity of 487 km s^{-1} and a long high-energy tail (Schwenn et al. 2006). We omit the few CMEs in this tail and the extremely low-velocity CMEs with $v_{\rm m} < 100$ km s^{-1}, attributing their range to that of the Alfvén speed. Applying the CME energy budget equation, we find that the range of V is 1100–2200 km s^{-1}. There is a remarkable overlap in the observed and predicted ranges.

4.5 Prediction of the CME rate

The phase-space ratio, measuring the fraction of catastrophe-prone states, can now be calculated and is found to be 0.046. The resulting predicted CME rate is 11 d^{-1}, higher than the true rate of 6 d^{-1} during solar maximum (Schwenn et al. 2006). However, the systematic uncertainties may be responsible for this discrepancy. The true range of velocities in the initial state is likely to be larger than that provided by current observations, because they cannot observe flows that are too slow or those that vary over relatively small regions. In addition, some of these DB catastrophes may result in a confined flare rather than a CME. Therefore, the predicted CME rate is in reasonable agreement with observations.

5 CONCLUSIONS AND DISCUSSION

In this paper, we have investigated whether solar eruptions could be produced by a catastrophic breakdown of the DB equilibrium of Hall MHD. Our main conclusions are given below.

(i) A catastrophe can occur in DB states that satisfy typical coronal conditions (i.e., a magnetically dominated state, with large-scale sizes much larger than the Hall scale).

(ii) This catastrophe converts up to half of the magnetic energy into kinetic energy; the released energy was shown to be large enough to drive a solar flare or CME.

(iii) The model predicts that the DB state's scale size expands by a factor of 2 or less as it evolves towards catastrophe, consistent with the kinematics of the quasi-equilibrium phase of LASCO C1 CMEs.

(iv) The predicted probability of an active region state being CME-prone is 0.046; taking active regions to correspond to DB states and estimating that new states appear every hour, this corresponds to a CME rate of 11 d^{-1}, which is reasonably close to the actual rate of 6 d^{-1}.

The DB model is extremely robust; for any region that is magnetically dominated, DB states will be the most likely equilibria if the Hall effect is more important than dissipation. Such regions include the magnetospheres of stars and accretion disc coronae. If observations indicate the existence of magnetically dominated, near-force-free states on a certain object, these observations are consistent with the presence of DB states. The DB model then provides a channel for eruptive or flaring events through the catastrophic breakdown of equilibrium.

Future work can make the DB model more physically realistic and detailed, allowing detailed comparison to observations. Because it is an equilibrium model, the DB model cannot predict the final destination of the energy released by the catastrophe or the detailed features of the post-equilibrium evolution. It is relatively easy to generalize the constant-density, purely magnetic model to compressible cases with an equation of state which include the effects of pressure variation and gravity (OSYM). By making this generalization and choosing an initial field geometry, it should be possible to determine if the DB catastrophe results in a CME, a confined flare or something else in a particular physical situation; this model can then be compared directly with observed solar events.

The DB equilibrium equations could also be applied directly to other stellar coronae, as well as to accretion disc coronae, which

have similar sub-Alfvénic flows and are magnetically dominated (Galeev, Rosner & Vaiana 1979). The DB equations provide a framework for creating detailed models of eruptive events on the Sun and other astrophysical objects.

ACKNOWLEDGMENTS

We are grateful to Daniel Gomez, Jesse Pino, Vinod Krishan and Nana Shatashvilli for comments and useful discussions. Daniel thanks his committee (Pawan Kumar, J. Craig Wheeler and Edward L. Robinson) for assisting him in this work.

REFERENCES

Aly J. J., 1991, ApJ, 375, L61
Bhattacharjee A., 2004, ARA&A, 42, 365
Chen J., 2001, Space Sci. Rev., 95, 165
Dasso S., Mandrini C. H., Démoulin P., Luoni M. L., Gulisano A. M., 2005, Adv. Space Res., 35, 711
Dennis B. R., Haga L., Medlin D. A., Tolbert A. K., 2006, BAAS, 38, 2
Emslie A. G., Dennis B. R., Holman G. D., Hudson H. S., 2005, J. Geophys. Res., 110, 11103
Forbes T. G. et al., 2006, Space Sci. Rev., 123, 251
Fredvik T., Kjeldseth-Moe O., Haugan S. V. H., Brekke P., Gurman J. B., Wilhelm K., 2002, Adv. Space Res., 30, 635
Galeev A. A., Rosner R., Vaiana G. S., 1979, ApJ, 229, 318
Gopalswamy N., Mikić Z., Maia D., Alexander D., Cremades H., Kaufmann P., Tripathi D., Wang Y.-M., 2006, Space Sci. Rev., 123, 303
Kjeldseth-Moe O., Brekke P., 1998, Sol. Phys., 182, 73
Krall J., Chen J., Santoro R., 2000, ApJ, 539, 964
Mahajan S. M., Yoshida Z., 1998, Phys. Rev. Lett., 81, 4863
Mahajan S. M., Miklaszewski R., Nikol'Skaya K. I., Shatashvili N. L., 2001, Phys. Plasmas, 8, 1340
Mahajan S. M., Shatashvili N. L., Mikeladze S. V., Sigua K. I., 2005, ApJ, 634, 419
Mewaldt R. A. et al., 2005, in Acharya B. S., Gupta S., Jagadeesan P., Jain A., Karthikeyan S., Morris S., Tonwar S., eds, 29th International Cosmic Ray Conference. Tata Institute of Theoretical Astrophysics, Mumbai, p. 129
Ohsaki S., Shatashvili N. L., Yoshida Z., Mahajan S. M., 2002, ApJ, 570, 395 (OSYM)
Schwenn R. et al., 2006, Space Sci. Rev., 123, 127
Sturrock P. A., 1991, ApJ, 380, 655
Woltjer L., 1958, Proc. Natl. Acad. Sci. USA, 44, 489
Zhang J., Dere K. P., Howard R. A., Kundu M. R., White S. M., 2001, ApJ, 559, 452

This paper has been typeset from a TEX/LATEX file prepared by the author.